URSI AP-RASC, Sydney, Australia, 17 – 22 August 2025

Complex Permittivity Imaging for Highly Non-linear Media for Microwave Breast Cancer Diagnosis

Shouhei Kidera[(1)] and Mutsuki Nakajima[(1)]
(1) Graduate School of Informatics and Engineering, University of Electro-Communications, Japan

Abstract

This paper introduces an accuracy enhanced a complex permittivity imaging for microwave breast cancer diagnosis, employing a background updating contrast source inversion (BU-CSI). The proposed method effectively mitigates inaccuracies caused by high non-linearity associated with high-contrast cancerous tissues by updating the background medium within the contrast source inversion (CSI) framework. The two-dimensional finite difference time domain (FDTD) based numerical tests demonstrate that our proposed method retains more accurate reconstruction, particularly in characterizing high-contrast cancerous regions.

1 Introduction

Breast cancer is the most prevailed and highest mortality cancer among women in the world. Microwave based diagnosis is promising as a more frequent screening technique because of lower energy exposure and less compressed measurement. The number of literature demonstrated that there are significant differences between cancerous and normal breast tissues in terms of complex permittivity in the microwave frequency band [1].

As a major imaging approach in microwave breast diagnosis, radar imaging scheme has been widely explored, however, they mostly suffers from strong clutter response from skin or healthy fibro-glandular tissues, leading to a high false positive rate. A nonlinear inverse scattering analysis, called as tomography, enables us to retrieve complex permittivity profile using scattered responses by solving the domain integral equation. However, its accuracy is significantly affected by the inherent nonlinearity and ill-posed nature of the problem, particularly when identifying high-contrast cancerous tissues. There are several studies to mitigate the non-linear problem, such as the levelset scheme [2], they needs predefined boundaries between low- and high-contrast regions based on prior knowledge of the dielectric properties of each tissue. Additionally, while some studies exploiting radar-based priors have been developed, these methods typically assume a vacuum background medium, which essentially suffers from inaccuracy due to non-linearity.

To address with the above-mentioned issue, especially for non-linearity, this paper introduce a background updating scheme in the contrast source inversion (CSI) scheme, where the background and its Green's function is sequentially updated by exploiting the optimization results of the original MF(Multiple Frequency)-CSI [3], namely, the total fields in the region of interest (ROI). The effectiveness of this method is validated through the two-dimensional (2-D) finite difference time domain (FDTD) method using a MRI-derived realistic numerical phantom.

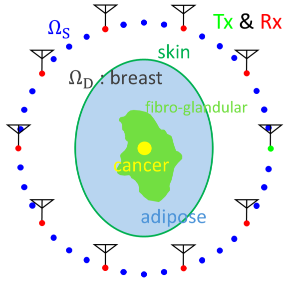

Figure 1. Observation model.

2 Method

The observation model is shown in Figure 1. Each tissue in breast (skin, adipose, fibro-glandular, cancer) is assumed to be lossy, dispersive dielectric property, which is located in the ROI as $\Omega_{\rm D}$. Multiple transmitting and receiving elements are placed around the breast. A total electric field from transmitter $r_{\rm T}$ to receiver $r_{\rm R}$ is expressed as $E^{\rm T}(\omega; r_{\rm T}, r_{\rm R})$ using an angular frequency ω.

The original CSI method [3] assumes a vacuum background medium, resulting in low estimation accuracy in high-contrast regions such as the mammary gland and cancerous tissue. To mitigate this issue, our proposed method updates the background medium, where the Green's function and the incident electric field for the updated background are determined by the total field optimized by the preliminary CSI results. Let background media $\tilde{\varepsilon}_{\rm B}(\omega; \boldsymbol{r})$, the scattered electric field is formulated as:

$$\begin{aligned}\tilde{E}^{\rm S}(\omega; r_{\rm T}, r_{\rm R}) &\equiv E^{\rm T}(\omega; r_{\rm T}, r_{\rm R}) - \tilde{E}^{\rm I}(\omega; r_{\rm T}, r_{\rm R}) \\ &= (\tilde{k}_{\rm B})^2 \int_{\Omega_{\rm D}} \tilde{G}^{\rm B}(\omega; r, r_{\rm R}) \tilde{w}(\omega; r_{\rm T}, r) dr \qquad (1)\end{aligned}$$

where $\tilde{E}^{\rm I}(\omega; r_{\rm T}, r_{\rm R})$ is the total electric field of the assumed background medium as $\tilde{\varepsilon}_{\rm B}(\omega; \boldsymbol{r})$. $\tilde{k}_{\rm B}$ and $\tilde{G}^{\rm B}(\omega; \boldsymbol{r}, \boldsymbol{r}_{\rm R})$ are the wavenumber and the Green's function of the given background medium. Notably, the CSI needs the two types of Green's functions in the data and state equations as $\tilde{G}^{\rm S}_{\rm B}(\omega; \boldsymbol{r}, \boldsymbol{r}_{\rm R})$ and $\tilde{G}^{\rm D}_{\rm B}(\omega; \boldsymbol{r}, \boldsymbol{r}')$, respectively, and the pro-

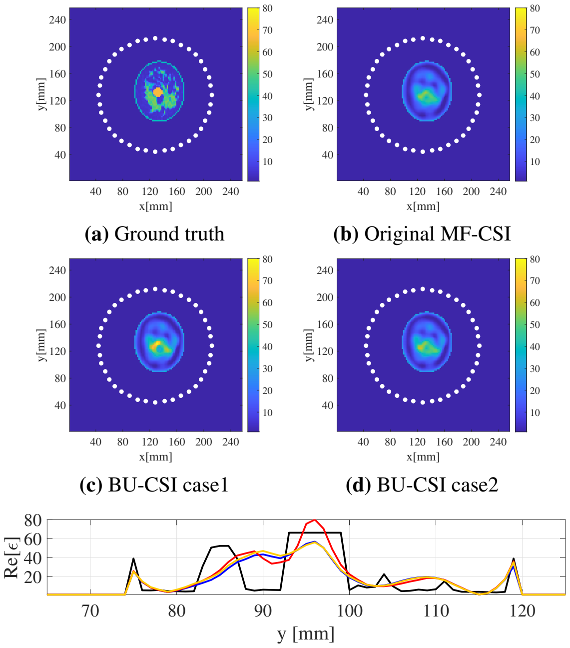

(a) Ground truth **(b)** Original MF-CSI **(c)** BU-CSI case1 **(d)** BU-CSI case2

(e) Cross-sectional view at $x = 132$ mm. (Black: Ground truth. Blue: Original MF-CSI. Red: BU-CSI case1. Yellow: BU-CSI case2).

Figure 2. Reconstruction results of real part of complex permittivity by each method @2.19 GHz.

posed method defines these Green's functions as:

$$\tilde{G}_{\mathrm{B}}^{\mathrm{S}}(\omega;\boldsymbol{r},\boldsymbol{r}_{\mathrm{R}}) \equiv \frac{\tilde{E}^{\mathrm{I}}(\omega;\boldsymbol{r}_{\mathrm{T}},\boldsymbol{r}_{\mathrm{R}})}{E^{\mathrm{I}}(\omega;\boldsymbol{r}_{\mathrm{T}},\boldsymbol{r}_{\mathrm{T}})} \quad (2)$$

$$\tilde{G}_{\mathrm{B}}^{\mathrm{D}}(\omega;\boldsymbol{r},\boldsymbol{r}') \equiv -\frac{i}{4}H_0^{(2)}(\bar{\tilde{k}}_{\mathrm{B}}|\boldsymbol{r}-\boldsymbol{r}'|),(\boldsymbol{r},\boldsymbol{r}' \in \Omega_{\mathrm{D}}) \quad (3)$$

where $H_0^{(2)}$ expresses the Hankel function of the second kind and zero-th order and $\bar{k}_{\mathrm{B}}$ denote an average wavenumber of background medium. $\tilde{w}(\omega;\boldsymbol{r}_{\mathrm{T}},\boldsymbol{r}) \equiv \chi(\omega;\boldsymbol{r})E^{\mathrm{T}}(\omega;\boldsymbol{r}_{\mathrm{T}},\boldsymbol{r}_{\mathrm{R}})$ and $\chi(\omega;\boldsymbol{r}) \equiv \frac{\varepsilon(r)-\varepsilon_{\mathrm{B}}(r;\omega)}{\varepsilon_{\mathrm{B}}(r;\omega)}$ are redefined. By updating $\tilde{\varepsilon}_{\mathrm{B}}(r,\omega)$ in the CSI with Eqs. (1), (3), and (3), a non-linear effect can be mitigated.

3 NUMERICAL RESULT

The numerical validations are presented using by the dispersive FDTD method to generate scattered data, where a realistic breast phantom in [4] is used. Here, a cancer tissue is placed in the center of the breast with 14 mm circle in size, and its Debye parameter is set to the 1.2 times of maximum values of fibroglandular tissue. The source current forms a raised cosine modulated pulse with a center frequency of 2.2 GHz and a bandwidth of 2.0 GHz. A circular array with 1 transmitter element and 9 receivers is rotated 360 degrees to obtain 40 samples in the angular direction. The Class 3 (high density) breast model with a cell size of 2 mm is assumed.

Figures 2 and 3 show the reconstruction results in each method. In the proposed method, the ideal condition where the total electric field and Green's function are provided by FDTD is Case # 1, and the condition where the CSI and

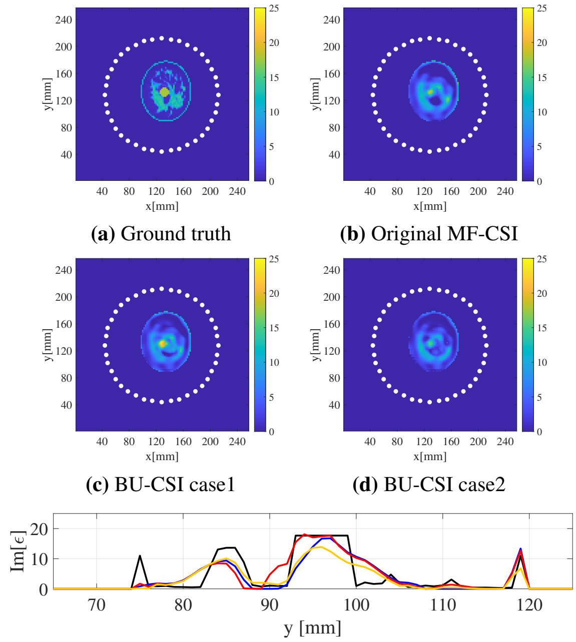

(a) Ground truth **(b)** Original MF-CSI **(c)** BU-CSI case1 **(d)** BU-CSI case2

(e) Cross-section image at $x = 132$ mm. (Black: Ground truth. Blue: Original MF-CSI. Red: BU-CSI case1. Yellow: BU-CSI case2).

Figure 3. Reconstruction results of imaginary part of complex permittivity by each method @2.19 GHz.

Table 1. RMSEs for complex permittivity reconstruction.

	Original MF-CSI	BU-CSI case1	BU-CSI case2
$\Re[\varepsilon]$	16.16	14.83	15.50
$\Im[\varepsilon]$	4.60	4.38	5.24

Hankel functions are given by CSI and Hankel functions as in equations3 and3 is Case # 2. The proposed method uses the background medium as a profile in the results of original MF-CSI, as in Fig. 2-(b) or 3-(b). Figure 2-(e) and 3-(e) also show the cross-sectional views at $x = 132$ mm, including the cancer. Table 1 show the root mean square error (RMSE) for real and imaginary parts of complex permittivity profile in fibro-glandular area. These results show that our proposed method provide more accurate reconstruction, particular in cancer existing area compared with those obtained by original MF-CSI method in cancer existing area.

4 CONCLUSION

This paper presents an accuracy enhanced complex permittivity imaging method for microwave breast cancer diagnosis using BU-CSI. The three-dimensional extension and experimental validations is our ongoing work.

References

[1] M. Lazebnik, *et al.*, *Phys. Med. Biol.*, vol.52, no.10, pp.2637-2656, May. 2007.

[2] T. J. Colgan, S. C. Hagness and B. D. Van Veen, *IEEE Trans. Biomed. Eng.*, vol. 62, no. 10, pp. 2526-2534, Oct. 2015.

[3] P. M. van Den Berg and A. Abubakar, *Progr. Electromagn. Res.*, vol.34, pp.189-218, 2001.

[4] URL : `http://uwcem.ece.wisc.edu`